

DRAFT VERSION APRIL 17, 2019

Typeset using L^AT_EX preprint style in AASTeX62

Dicarbon formation in collisions of two carbon atoms

JAMES F. BABB,¹ R. T. SMYTH,^{1,2} AND B. M. MCLAUGHLIN^{1,2}

¹*Institute for Theoretical Atomic, Molecular, and Optical Physics,*

Center for Astrophysics | Harvard & Smithsonian, 60 Garden St., Cambridge, MA 02138

²*Centre for Theoretical Atomic, Molecular, and Optical Physics, School of Mathematics & Physics*

Queen's University of Belfast, Belfast BT7 1NN, Northern Ireland, UK

(Dated: Accepted 2019 March 14)

ABSTRACT

Radiative association cross sections and rates are computed, using a quantum approach, for the formation of C₂ molecules (dicarbon) during the collision of two ground state C(³P) atoms. We find that transitions originating in the C ¹Π_g, d ³Π_g, and 1 ⁵Π_u states are the main contributors to the process. The results are compared and contrasted with previous results obtained from a semi-classical approximation. New *ab initio* potential curves and transition dipole moment functions have been obtained for the present work using the multi-reference configuration interaction approach with the Davidson correction (MRCI+Q) and aug-cc-pCV5Z basis sets, substantially increasing the available molecular data on dicarbon. Applications of the current computations to various astrophysical environments and laboratory studies are briefly discussed focusing on these rates.

Keywords: molecular processes — molecular data — interstellar chemistry

1. INTRODUCTION

Dicarbon (C₂) was first observed spectroscopically in flames and arcs and continues to be a useful diagnostic there, and in carbon plasmas for other laboratory and industrial applications (Nemes & Irle 2011). The molecule has been observed in a host of extraterrestrial sources such as comets, carbon stars, protoplanetary nebulae, and molecular clouds.

Interstellar dicarbon has been detected at optical wavelengths in diffuse (Chaffee & Lutz 1978; van Dishoeck et al. 1993; Gredel et al. 2001) and translucent (van Dishoeck & Black 1989; Iglesias-Groth 2011) molecular clouds. The optical detection of C₂ in comets is an element of their classification into “typical” and “depleted” (A’Hearn et al. 1995; Cochran et al. 2012). Dicarbon is present in solar (Lambert 1978) and model stellar atmospheres, including the pioneering work of Tsuji (1964)

jbabb@cfa.harvard.edu

rsmyth41@qub.ac.uk

bmclaughlin899@btinternet.com

and Lord (1965), and seen, for example, in solar optical (Grevesse & Sauval 1973) and infrared spectra (Brault et al. 1982) and in infrared spectra of carbon-rich giant stars (Goebel et al. 1983; Loidl et al. 2001). The presence of the Swan bands of dicarbon (optical wavelengths) is an important element in the classification scheme of carbon stars (Keenan 1993; Green 2013). The mechanisms of formation of dicarbon vary, depending on the operative chemistries: For example, in diffuse molecular clouds dissociative recombination of CH_2^+ leads to C_2 (Black & Dalgarno 1977; Federman & Huntress 1989), while in comets a chemistry starting with photodissociation of C_2H_2 or C_2H may be operative (Jackson 1976).

Of particular interest for the present work is the formation of carbonaceous dust in the ejecta of core-collapse supernovae, where the formation of dicarbon through radiative association enters chemical models (Liu et al. 1992; Cherchneff & Dwek 2009; Clayton & Meyer 2018; Sluder et al. 2018) and is an initial step in models of formation of larger carbon clusters through condensation (Clayton et al. 1999; Clayton et al. 2001; Clayton 2013) or nucleation (Lazzati & Heger 2016). [Later, in Sec. 4, we discuss in more detail laboratory experiments on carbon vapors generated by laser radiation. We note at this point that evidence of associative collisions of two ground state carbon atoms was found by Monchicourt (1991) in light emission from laser-induced expansion of carbon vapor from a graphite rod.] Fig. 1 illustrates a sample of the experimentally observed bands (Tanabashi et al. 2007; Bornhauser et al. 2015; Macrae 2016; Furtenbacher et al. 2016) connecting eleven singlet, triplet, and quintet states of the C_2 molecule that contribute to the overall radiative association rate coefficient for this molecule. In the ejecta of SN1987A and other core-collapse supernovae, CO and SiO were detected, see (Cherchneff & Sarangi 2011; Sarangi et al. 2018), through fundamental ($\Delta\nu = 1$) bands¹ of ground molecular electronic states allowing observational tests of molecular formation models (Liu et al. 1992; Liu & Dalgarno 1995; Cherchneff & Sarangi 2011; Sarangi & Cherchneff 2013; Rho et al. 2018)—dicarbon, however, lacks a permanent electric dipole moment and analogous vibrational transitions (fundamental bands) do not exist, making reliable theoretical predictions of rate coefficients imperative. Moreover, recent three-dimensional mapping of CO and SiO in the SN 1987A core ejecta with the Atacama Large Millimeter/submillimeter Array (ALMA) shows a clumpy mixed structure calling for improvements beyond one-dimension in hydrodynamical and chemical modeling of molecular formation (Abellán et al. 2017); a reliable description of dicarbide formation might improve such future calculations. Finally, understanding the origins of cosmic dust and the roles played by supernovae in contributing to extragalactic dust depends on progress in modeling dust formation (Sarangi et al. 2018; Sluder et al. 2018).

The radiative association (RA) rate was originally estimated to have a rate coefficient $k_{\text{C}_2} \approx 1 \times 10^{-17} \text{ cm}^3/\text{s}$ (Prasad & Huntress 1980; Millar et al. 1991) for theoretical models of interstellar clouds and subsequent semi-classical calculations (Andreazza & Singh 1997) found comparable values with a weak temperature dependence increasing from $3.07 \times 10^{-18} \text{ cm}^3/\text{s}$ at 300 K to $1.65 \times 10^{-17} \text{ cm}^3/\text{s}$ at 14,700 K. In recent studies using a quantum approach on systems such as SiP (Golubev et al. 2013), SiO (Forrey et al. 2016; Cairnie et al. 2017) and CS (Pattillo et al. 2018; Forrey et al. 2018), it was found that the semi-classical calculations (Andreazza & Singh 1997; Andreazza et al. 2006) underestimated the cross sections and rates, particularly at low temperatures.

¹ CO was also detected in the first overtone band ($\Delta\nu = 2$). In SN 1987A individual rotational lines of CO and of SiO were detected at late epoch, see Abellán et al. (2017); Sarangi et al. (2018).

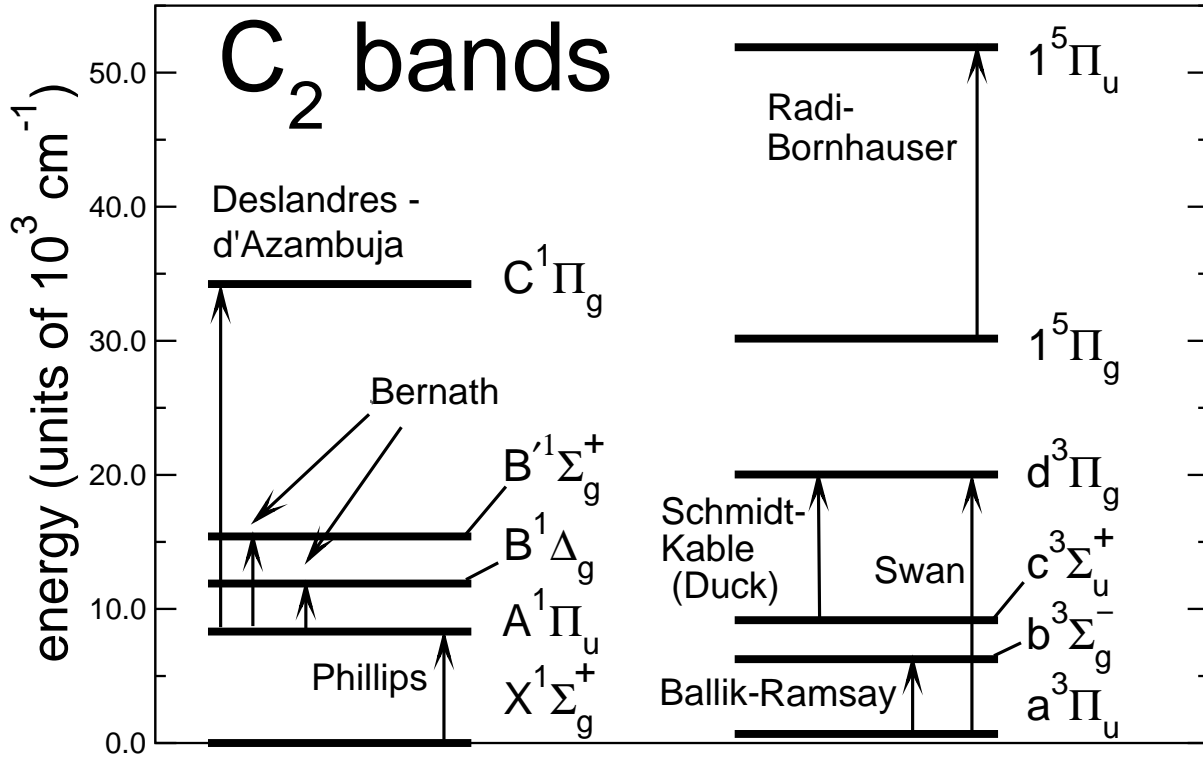


Figure 1. Experimentally observed C_2 band systems connecting eleven singlet, triplet, and quintet electronic states dissociating to ground state carbon atoms; schematic illustration of electronic state term energies T_e in cm^{-1} calculated in the present work [after Messerle & Krauss (1967); Tanabashi et al. (2007); Bornhauser et al. (2015); Macrae (2016); Furtenbacher et al. (2016)].

In the present study we obtain results from a quantum approach to estimate the cross sections and rate coefficients for C_2 formation by radiative association using new highly accurate ab initio molecular data for the potential energy curves (PEC's) and transition dipole moments (TDM's) coupling the states of interest. Results from our present quantum approach are compared with the previous semi-classical results of [Andreazza & Singh \(1997\)](#) and conclusions are drawn.

The layout of this paper is as follows. An overview of how the molecular data is obtained for our dynamical calculations is presented in [section 2](#). In [section 3](#), a brief overview of the radiative association cross section and rates are outlined. The computed radiative association cross sections, and rates are presented in [section 3](#) and are compared with the previous semi-classical work of [Andreazza & Singh \(1997\)](#) in [section 4](#). Finally in [section 5](#) conclusions are drawn from our work. Atomic units are used throughout unless otherwise specified.

2. THEORY AND CALCULATIONS

2.1. Potential Curves and Transition Dipole Moments

In a similar manner to our recent all electron molecular structure and resulting dynamical studies on diatomic systems such as: SiO (Forrey et al. 2016; Cairnie et al. 2017), CS (Pattillo et al. 2018; Forrey et al. 2018), HeC⁺ (Babb & McLaughlin 2017a), SH⁺ (Shen et al. 2015; McMillan et al. 2016), CH⁺ (Babb & McLaughlin 2017b), and HeAr⁺ (Babb & McLaughlin 2018), the potential energy curves (PECs) and transition dipole moments (TDMs) for the eighteen singlet, triplet and quintet electronic states are calculated within an MRCI+Q approximation for the approach of ground state carbon atoms. That is, we use a state-averaged-multi-configuration-self-consistent-field (SA-MCSCF) approach, followed by multi-reference configuration interaction (MRCI) calculations together with the Davidson correction (MRCI+Q) (Helgaker et al. 2000). The SA-MCSCF method is used as the reference wave function for the MRCI calculations. Low-lying singlet, triplet and quintet electronic states and the transition dipole matrix elements connecting these molecular states are calculated and used in the present dynamical calculations for the radiative association process. The literature on the molecular properties of dicarbon is extensive; sources with comprehensive bibliographies include Martin (1992); Nemes & Irle (2011); Zhang et al. (2011); Boschen et al. (2014); Macrae (2016); Furtenbacher et al. (2016); Yurchenko et al. (2018); Varandas & Rocha (2018).

Potential energy curves and transition dipole moments as a function of internuclear distance R are calculated starting from a bond separation of $R = 1.5$ Bohr extending out to $R = 20$ Bohr. The basis sets used in the present work are the augmented correlation consistent polarized core valence quintuplet [aug-cc-pcV5Z (ACV5Z)] Gaussian basis sets. The use of such large basis sets is well known to recover 98% of the electron correlation effects in molecular structure calculations (Helgaker et al. 2000). All the PEC and TDM calculations for the C₂ molecule were performed with the quantum chemistry program package MOLPRO 2015.1 (Werner et al. 2015), running on parallel architectures.

For molecules with degenerate symmetry, an Abelian subgroup is required to be used in MOLPRO. So for a diatomic molecule like C₂ with D_{∞h} symmetry, it will be substituted by D_{2h} symmetry with the order of irreducible representations being ($A_g, B_{3g}, B_{2g}, B_{1g}, B_{1u}, B_{2u}, B_{3u}, A_u$). When symmetry is reduced from D_{∞h} to D_{2h}, (Herzberg 1950) the correlating relationships are $\sigma_g \rightarrow a_g$, $\sigma_u \rightarrow a_u$, $\pi_g \rightarrow (b_{2g}, b_{3g})$, $\pi_u \rightarrow (b_{2u}, b_{3u})$, $\delta_g \rightarrow (a_g, b_{1g})$, and $\delta_u \rightarrow (a_u, b_{1u})$.

In order to take account of short-range interactions, we employed the non-relativistic state-averaged complete active-space-self-consistent-field (SA-CASSCF)/MRCI method available within the MOLPRO (Werner et al. 2012, 2015) quantum chemistry suite of codes.

For the C₂ molecule, molecular orbitals (MOs) are put into the active space, including ($3a_g, 1b_{3u}, 1b_{2u}, 0b_{1g}, 3b_{1u}, 1b_{2g}, 1b_{3g}, 0a_u$), symmetry MOs. The molecular orbitals for the MRCI procedure were obtained using the SA-MCSCF method, for singlet and triplet spin symmetries, we carried out the averaging processes on the two lowest states of the symmetries; ($A_g, B_{3u}, B_{1g}, B_{1u}$) and the lowest states of the symmetries; (B_{2u}, B_{3g}, B_{2g} and A_u). A similar approach was also used for the quintet states. This approach provides an accurate representation of the singlet, triplet and quintet states of interest as the molecule dissociated.

At bond separations beyond $R = 14$ Bohr, the PECs are smoothly fitted to functions of the form

$$V(R) = \frac{C_5}{R^5} - \frac{C_6}{R^6}, \quad (1)$$

where for the particular electronic state, C_5 is the quadrupole-quadrupole electrostatic interaction (Knipp 1938; Chang 1967) and C_6 is the dipole-dipole dispersion (van der Waals) coefficient (we use atomic units unless otherwise specified). For $R < 1.5$ Bohr, short-range interaction potentials of the form $V(R) = A \exp(-BR) + C$ are fitted to the *ab initio* potential curves. Estimates of the values of the quadrupole-quadrupole coefficients C_5 were given by Knipp (1938), and by Boggio-Pasqua et al. (2000) (for singlet and triplet Σ , Π and Δ electronic states, which suffices to determine those for quintet states by symmetry). The long range dispersion coefficient C_6 (averaged over the possible fine structure levels of two carbon atoms) was calculated to be 40.9 ± 4.4 using many-body perturbation theory by Miller & Kelly (1972) and estimated to be 46.29 using the London formula by Chang (1967). In fitting the long-range form Eq. (1) to the calculated potential energy data, we adjusted the values of C_5 and C_6 , as necessary to match the slopes of the potential energy curves. The adopted values are given in Table 1. We began with estimates of C_5 from Knipp (1938) and Boggio-Pasqua et al. (2000) and limited our adjustment of C_6 to either the value of Miller & Kelly (1972) or that of Chang (1967). For the $B^1\Sigma_g^+$ state, there is a barrier in the potential energy curve (0.0086 eV or 69 cm^{-1} at $R = 7.12$), reflected in the positive value of C_5 which fit the data. This is in good accord with a value found by Varandas (2008), 43 cm^{-1} at $R = 8.37$, in an extensive study of diabatic representations of the $X^1\Sigma_g^+$ and $B^1\Sigma_g^+$ states. (This barrier energy is too low to appreciably affect the dynamics calculations presented below.)

As a consequence of fitting the potentials to Eq. (1), the calculated potentials (as output from MOLPRO) were shifted. In Table 1 we list the final values of T_e (in cm^{-1}) relative to the minimum of the $X^1\Sigma_g^+$ potential energy curve and the term energies are plotted schematically in Fig. 1 for experimentally observed bands. Our calculated values may be compared with the recent experimental fits in Table 4, column 3, of Furtenbacher et al. (2016), and we agree to within 100 cm^{-1} for the $a^3\Pi_u$, $A^1\Pi_u$, $c^3\Sigma_u^+$, and $B^1\Delta_g$ states, and to within 205 cm^{-1} for the $b^3\Sigma_g^-$ and $B^1\Sigma_g^+$ states. For the $1^5\Pi_g$ state, our value of T_e is within 9 cm^{-1} of the *ab initio* value given by Schmidt & Bacskay (2011) (expressed with respect to the minimum of the $a^3\Pi_u$ curve and calculated using the aug-cc-pV5Z basis sets). Our calculated $1^5\Pi_u$ state supports a shallow well in agreement with previous calculations (Bruna & Grein 2001; Bornhauser et al. 2015; Visser et al. 2019), deepening the shelf-like form of the curve found in the earlier calculations of Kirby & Liu (1979). The accuracy of the present potential energy curves is very satisfactory for the purposes of the present study. The potential curves for C_2 singlet, triplet and quintet states are shown in Fig. 2. Structures due to nonadiabatic couplings are apparent in the $c^3\Sigma_u^+$ and $2^3\Sigma_u^+$ curves due to their mutual interaction and interactions with higher states (see Fig. 3 of Kirby & Liu (1979)). As we will show below, the calculated cross sections involving the $c^3\Sigma_u^+$ and $2^3\Sigma_u^+$ states are several orders of magnitude smaller than those from the leading transitions contributing to the total radiative association cross sections. Similar structures in the quintet states (Bruna & Grein 2001) occur at energies at about 1 eV corresponding to kinetic temperatures above the range of the present study. Thus, we ignore nonadiabatic couplings and expect that they will have at most a minor effect on the net total cross sections for radiative association.

The TDMs for the C_2 molecule are similarly extended to long- and short-range internuclear distances. For $R > 14$ a functional fit of the form $D(R) = a \exp(-bR) + c$ is applied, while in the short range $R < 1.5$ a quadratic fit of the form $D(R) = a'R^2 + b'R + c'$ is adopted. The TDMs for singlet transitions are shown in Fig. 3, for triplet transitions in Fig. 4, and for quintet transitions in Fig. 5.

Table 1. The eighteen C_2 , singlet, triplet and quintet electronic states formed during the collision of two ground state carbon atoms. In column 2 the values of the term energies T_e are listed for the potential energies fit to Eq. (1) relative to the minimum of the $X^1\Sigma_g^+$ potential energy. For each electronic state used in the present work, we list in atomic units values of C_5 from Boggio-Pasqua et al. (2000) and the adopted values of C_5 and C_6 entering Eq. (1). The states $1^1\Sigma_u^-$, $1^5\Delta_g$, and $1^5\Sigma_u^-$ were not fitted in the present work, so we list the values of T_e as calculated *ab initio* for $1^1\Sigma_u^-$ and $1^5\Delta_g$, while $1^5\Sigma_u^-$ is repulsive.

State	T_e (cm ⁻¹) ^a	C_5^b	C_5^c	C_6^d
X $1^1\Sigma_g^+$	0.0	21.81	5	40.9
A $1^1\Pi_u$	8312.4	0	0	46.29
B $1^1\Delta_g$	11895	3.635	3.635	46.29
B' $1^1\Sigma_g^+$	15205	0	16	40.29
C $1^1\Pi_g$	34231	-14.54	-13.49	40.9
1 $1^1\Sigma_u^-$	39500	0		
a $3^1\Pi_u$	678.74	-14.54	-14.54	46.29
b $3^1\Sigma_g^-$	6254.9	0	0	40.9
c $3^1\Sigma_u^+$	9157.5	21.81	5	40.9
d $3^1\Pi_g$	20031	0	0	46.29
2 $3^1\Sigma_u^+$	40042	0	0	40.9
1 $3^1\Delta_u$	41889	3.635	8	46.29
1 $5^1\Pi_g$	30165	-14.54	-13.49	40.9
1 $5^1\Sigma_g^+$	40197	0	0	40.9
1 $5^1\Pi_u$	51897	0	0	46.29
2 $5^1\Sigma_g^+$	64088	21.81	12	40.29
1 $5^1\Delta_g$	49900	3.635		
1 $5^1\Sigma_u^-$		0		

^aPresent calculations.

^bSinglet and triplet values from Boggio-Pasqua et al. (2000), quintet values by symmetry. See text for details.

^cActual value used. See text for details.

^dEstimated from Miller & Kelly (1972) or Chang (1967). See text for details.

As shown in Figs. 3 and 4 the results are in satisfactory agreement with previous calculations for the Phillips, Swan, Ballik-Ramsay, and Schmidt-Kable (Duck) bands (Oneil et al. 1987; Langhoff et al.

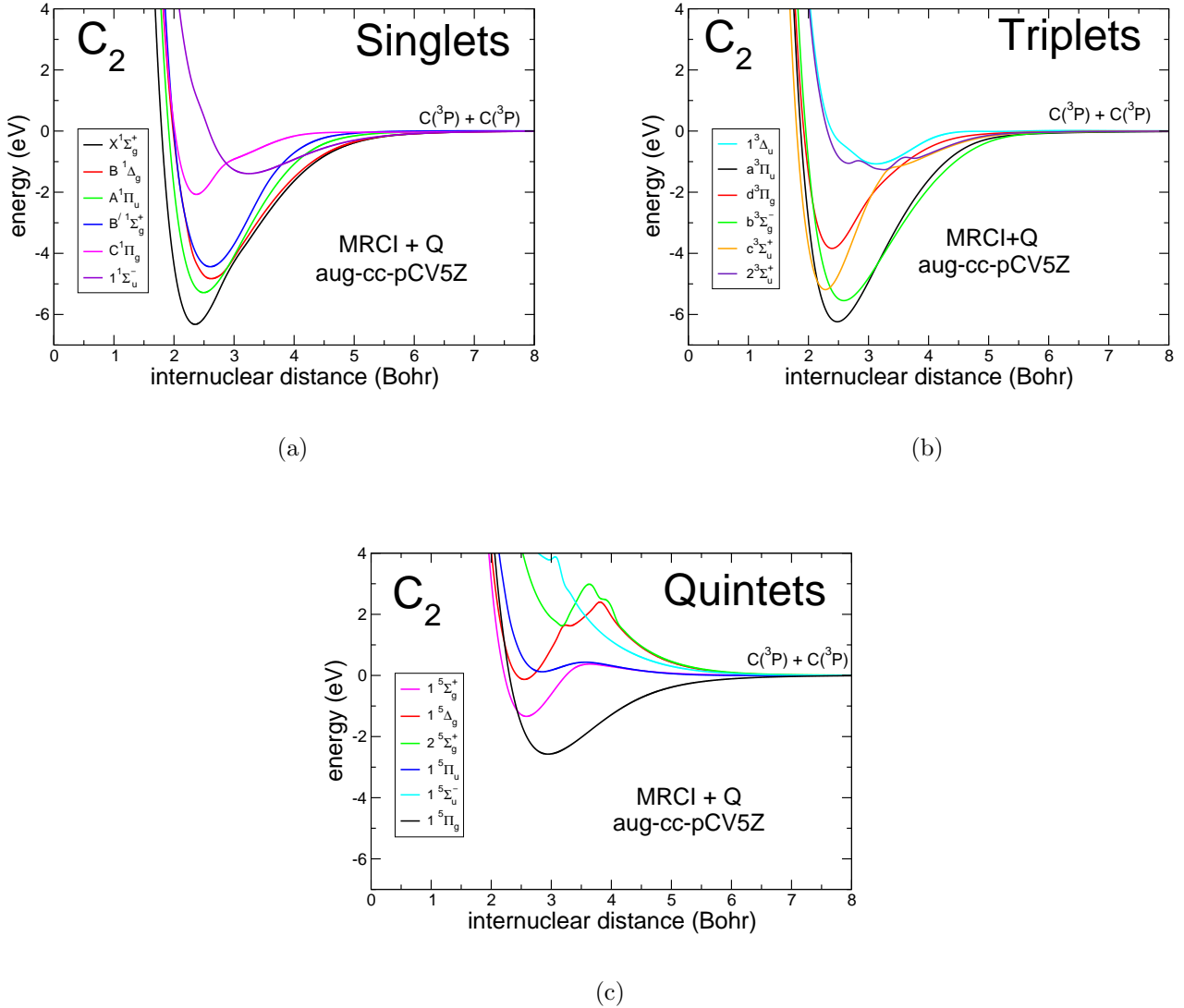


Figure 2. Potential energy curves (eV), as a function of internuclear distance (Bohr) for C_2 molecular states dissociating to ground state carbon atoms, (a) singlet, (b) triplet, and (c) quintet states. Results were obtained using the quantum chemistry package MOLPRO and aug-cc-pCV5Z basis for each atom.

1990; Kokkin et al. 2007; Brooke et al. 2013). In addition, our results for the Bernath $B'\Sigma_g^+ - A^1\Pi_u$ and Deslandres-d’Azambuja bands are provided over a substantially larger range of internuclear distances compared to the earlier MRDCI calculations of Chabalowski et al. (1983). (The band $1^5\Sigma_g^+ - 1^5\Pi_u$ has not yet been observed (Bornhauser et al. 2015); we point out that $2^3\Sigma_u^+ - d^3\Pi_g$, $1^3\Delta_u - d^3\Pi_g$, and $1^5\Delta_g - 1^5\Pi_u$ bands may exist. Additionally, we observe that the $2^3\Sigma_u^+ - d^3\Pi_g$ band might contribute at wave numbers where significant spectral congestion is seen in dicarbon (Tanabashi et al. 2007).)

3. CROSS SECTIONS

The quantum mechanical cross section for the radiative association process $\sigma_{i \rightarrow f}^{\text{QM}}(E)$, where the initial i and final f electronic states are labeled by their molecular states (e.g. $d^3\Pi_g$) can be calculated

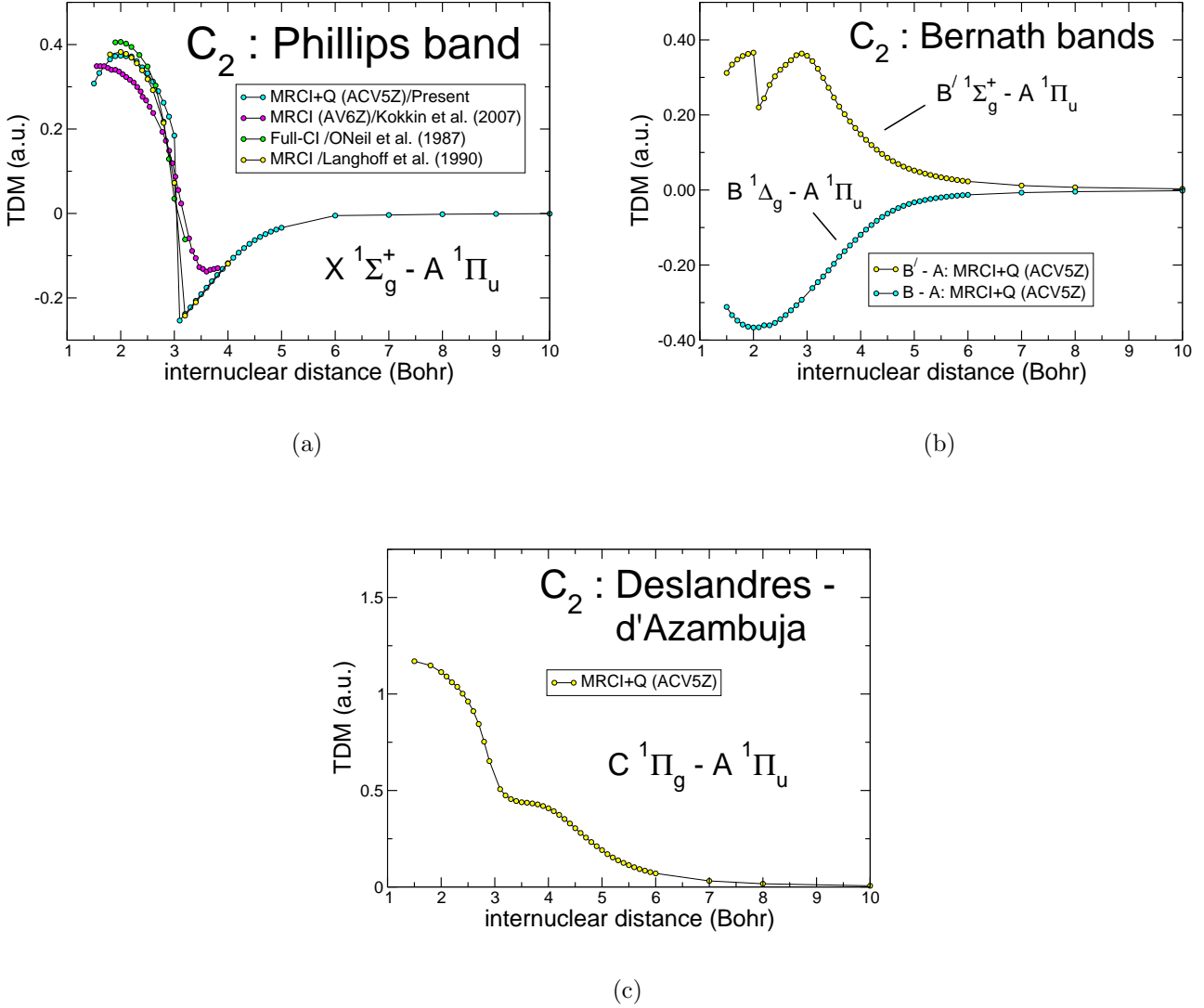


Figure 3. Transition dipole moments (TDMs) for singlet transitions in C_2 in atomic units, (a) Phillips band ($A^1\Pi_g - X^1\Sigma_g^+$), (b) Bernath bands ($B^1\Delta_g - A^1\Pi_u$ and $B'^1\Sigma_g^+ - A^1\Pi_u$) and (c) Deslandres-d'Azambuja band ($C^1\Pi_g - A^1\Pi_u$). For the Phillips band we compare the present MRCI+Q work with results from ONeil et al. (1987); Langhoff et al. (1990) and Kokkin et al. (2007).

using perturbation theory (see, for example, (Babb & Dalgarno 1995; Gianturco & Gori Giorgi 1996) and (Babb & Kirby 1998)). The result is

$$\sigma_{i \rightarrow f}^{QM}(E) = P_i \sum_{v'J'} \sum_J \frac{64}{3} \frac{\pi^5}{137.036^3} \frac{\nu^3}{2\mu E} \mathcal{S}_{JJ'} |M_{iEJ, f v' J'}|^2, \quad (2)$$

where the sum is over initial partial waves with angular momenta J and final vibrational v' and rotational J' quantum numbers, $\mathcal{S}_{JJ'}$ are the appropriate line strengths (Cowan 1981; Curtis 2003) or Hönl-London factors (Watson 2008), 137.036 is the speed of light in atomic units, μ is the reduced

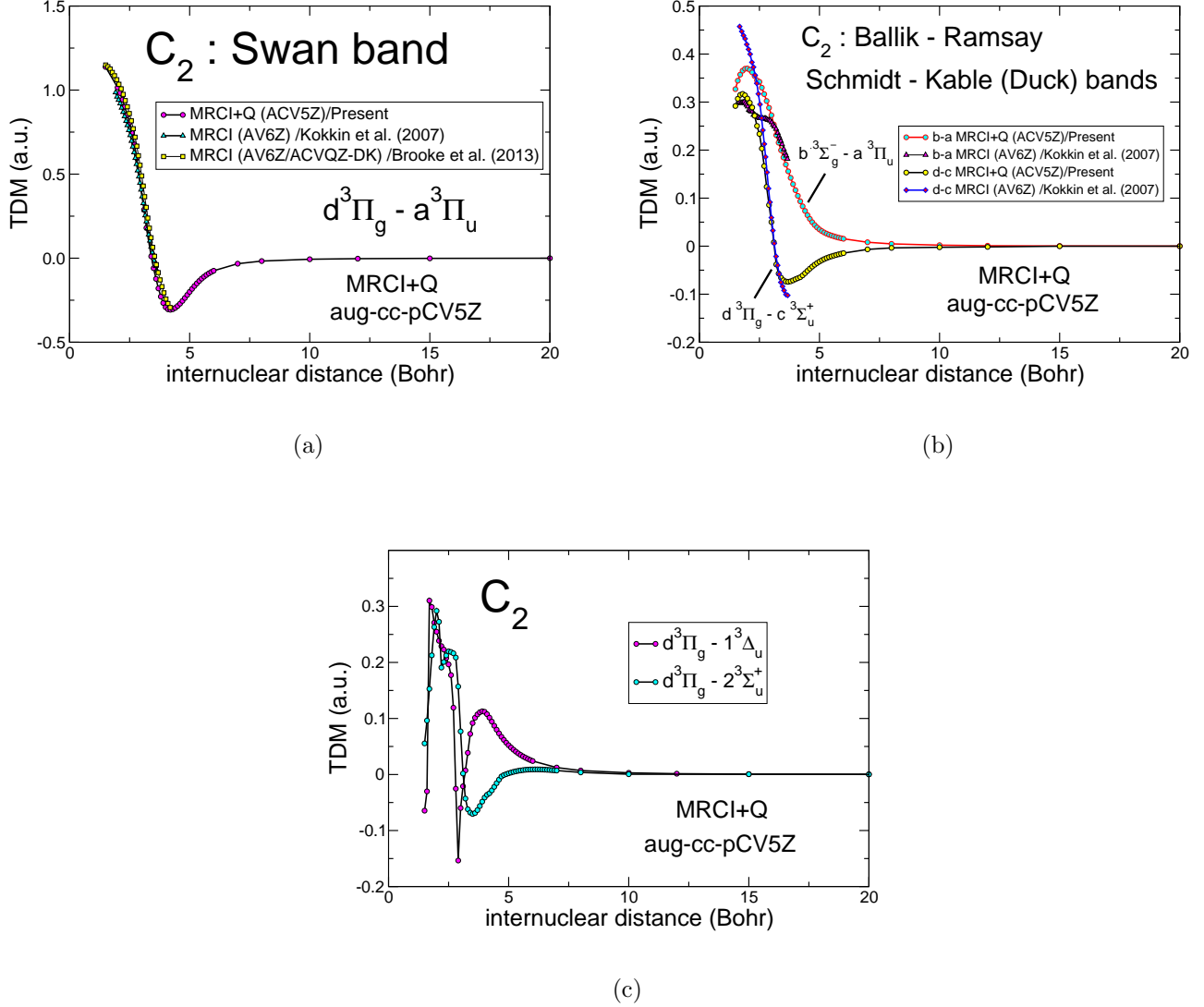


Figure 4. Transition dipole moments for triplet transitions in C_2 in atomic units, (a) Swan band ($d^3\Pi_g - a^3\Pi_u$), (b) Ballik-Ramsay ($b^3\Sigma_g^- - a^3\Pi_u$), and the Schmidt-Kable (Duck) bands ($d^3\Pi_g - c^3\Sigma_u^+$). Other triplet transition dipole moments are shown in (c) for the ($d^3\Pi_g - 1^3\Delta_u$) and the ($d^3\Pi_g - 2^3\Sigma_u^+$) bands. We compare the present MRCI+Q work with results from [Kokkin et al. \(2007\)](#) for the Swan and Ballik-Ramsay bands and from [Brooke et al. \(2013\)](#) for the Swan band.

mass of the collision system, and $M_{iEJ,fv'J'}$ is given by the integral

$$M_{iEJ,fv'J'} = \int_0^\infty F_{iEJ}(R) D_{if}(R) \Phi_{fv'J'}(R) dR. \quad (3)$$

The wave function $\Phi_{\Lambda'v'J'}(R)$ is a bound state wave function of the final electronic state, $F_{\Lambda EJ}(R)$ is an energy-normalized continuum wave function of the initial electronic state, and $D_{if}(R)$ is an electric dipole transition dipole moment between i and f .

Due to presence of identical nuclei and the absence of nuclear spin in $^{12}C_2$, the rotational quantum numbers of the $^1\Sigma_g^+$ states are even and for any given value of $\Lambda = 1$ or 2 , only one lambda-doubling

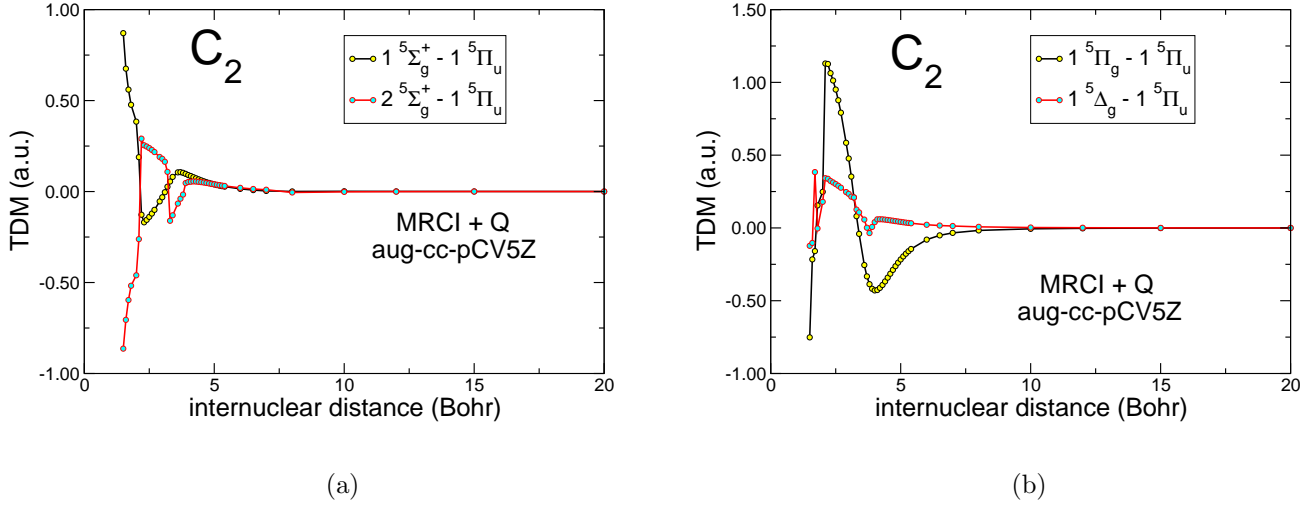


Figure 5. Transition dipole moments for quintet transitions in C_2 in atomic units, (a) ($1^5\Sigma_g^+ - 1^5\Pi_u$) and the ($2^5\Sigma_g^+ - 1^5\Pi_u$) bands, and in (b) for the ($1^5\Pi_g - 1^5\Pi_u$), and ($1^5\Delta_g - 1^5\Pi_u$) bands.

level is populated (Amiot 1983). Thus, the statistical weight factor P_i is given by

$$P_i = (2S_i + 1)/81, \quad (4)$$

where S_i is the total spin of the initial molecular electronic state (here 1, 3, or 5), and there are for two $C(^3P)$ atoms $3^4 = 81$ molecular states labeled by Λ and S . Thus, for example, for the $^{12}C_2$ molecule considered here, $P_i = \frac{1}{81}$, $\frac{3}{81}$ or $\frac{5}{81}$, respectively, for $i = A^1\Pi_u$, $b^3\Sigma_g^+$, or $1^5\Pi_g$.

Table 2. Transitions studied in this work. Listed in order of decreasing contribution to total cross section.

Initial	Final	Band Name
C $1^1\Pi_g$	A $1^1\Pi_u$	Deslandres-d'Azambuja
d $3^3\Pi_g$	a $3^3\Pi_u$	Swan
1 $5^5\Pi_u$	1 $5^5\Pi_g$	Radi-Bornhauser
2 $3^3\Sigma_u^+$	d $3^3\Pi_g$...
1 $3^3\Delta_u$	d $3^3\Pi_g$...
b $3^3\Sigma_g^-$	a $3^3\Pi_u$	Ballik-Ramsey
d $3^3\Pi_g$	c $3^3\Sigma_u^+$	Schmidt-Kable
A $1^1\Pi_u$	X $1^1\Sigma_g^+$	Phillips
B' $1^1\Sigma_g^+$	A $1^1\Pi_u$	Bernath B'
B $1^1\Delta_g$	A $1^1\Pi_u$	Bernath B
2 $5^5\Sigma_g^+$	1 $5^5\Pi_u$...

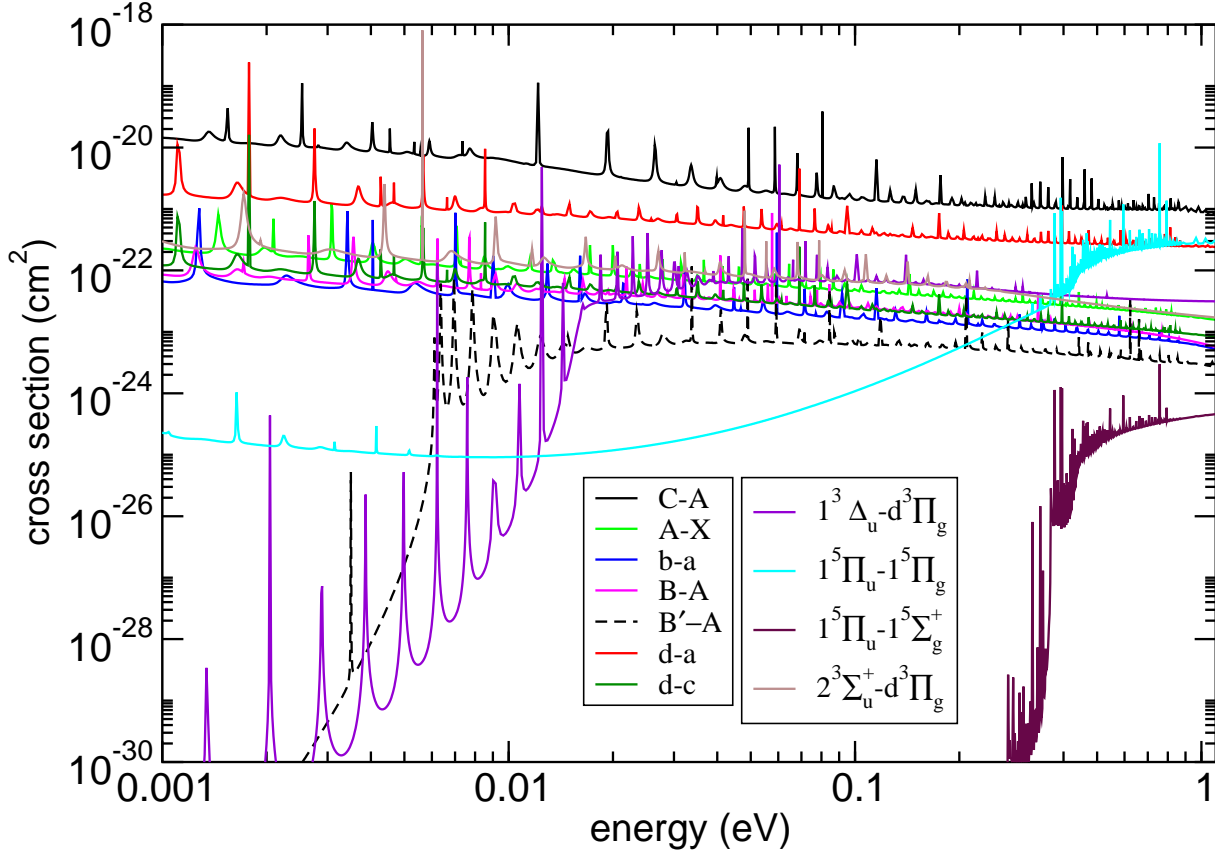


Figure 6. Radiative association cross sections (units of cm^2) as a function of the collision energy E (eV) for the collision of two $^{12}\text{C}(^3P)$ atoms. Results are shown for the singlet, triplet, and quintet transitions listed in Table 2. In order to gauge the cross sections, all data are plotted with the statistical factor $P_i = 1$. We see that the Deslandres-d’Azambuja ($C^1\Pi_g-A^1\Pi_u$), Swan ($d^3\Pi_g-a^3\Pi_u$) and Radi-Bornhauser ($1^5\Pi_u-1^5\Pi_g$) bands have the largest cross sections.

The bound and continuum state wave functions may be computed from their respective Schrödinger equations using the grid-based approach of the Numerov method (Cooley 1961; Johnson 1977), where we used step sizes of up to 0.001 Bohr. For example, for the $X^1\Sigma_g^+$ state, we find 55 vibrational levels and $J = 0, 2, \dots, 174$, though not all levels will contribute to the cross sections. A finely spaced energy grid is required to account for resonances. In Fig. 6, results are shown for the radiative association cross section as a function of energy for the singlet, triplet, and quintet transitions listed in Table 2. We plot the cross sections with the statistical factor P_i set equal to unity for all states. Numerous shape resonances are visible. For the $1^3\Delta_u-d^3\Pi_g$ and $1^5\Pi_u-1^5\Pi_g$ cross sections, resonance tunneling features are visible, corresponding to potential barriers (local maxima) in the entrance channels. The local maxima from the potential energy curves are 0.015 eV at $R = 6$ for $1^3\Delta_u$, 0.37 eV at $R = 3.6$ for $2^5\Sigma_g^+$, and 0.42 eV at $R = 3.5$ for $1^5\Pi_u$ and as seen in Fig. 6 the corresponding

cross sections sharply diminish for collision energies below these values. Note, the cross sections for Deslandres-d’Azambuja transitions ($C^1\Pi_g-A^1\Pi_u$) dominate the other cross sections for all collision energies, followed by the cross sections for the Swan ($d^3\Pi_g-a^3\Pi_u$) transitions. The cross sections for Radi-Bornhauser transitions ($1^5\Pi_u-1^5\Pi_g$) rise sharply as the relative energy increases. The other cross sections are at least an order of magnitude weaker than those corresponding to Deslandres-d’Azambuja, Swan, and Radi-Bornhauser transitions and will not contribute significantly to the total cross section. While the $1^5\Pi_u$ state does support some bound levels (Bornhauser et al. 2017), the calculated cross sections from the $2^5\Sigma_g^+-1^5\Pi_u$ state are negligible because of the steeply repulsive tail of the initial $2^5\Sigma_g^+$ electronic state.

3.1. Rate Constant

The potential energy curves and transition dipole moments were then used to calculate the cross sections and rates for radiative association in the C_2 molecule. The thermal rate constant (in cm^3s^{-1}) at a given temperature T to form a molecule by radiative association is given by

$$k_{i\rightarrow f} = \left(\frac{8}{\mu\pi}\right)^{1/2} \left(\frac{1}{k_B T}\right)^{3/2} \int_0^\infty E \sigma_{i\rightarrow f}(E) e^{-E/k_B T} dE, \quad (5)$$

where k_B is Boltzmann’s constant.

The complicated resonance structures make it challenging to calculate accurately the rate coefficient using numerical integration (Bennett et al. 2003; Gustafsson et al. 2012). As a guide, the relationship $v\sigma_{i\rightarrow f}^{\text{QM}}$, where $v = \sqrt{2E/\mu}$, is used to designate an effective energy-dependent rate coefficient, where $R(E)$ for a transition from state i to state f is given by,

$$R(E) = \sqrt{2E/\mu} \sigma_{i\rightarrow f}^{\text{QM}}(E) \quad (6)$$

This form is often used to define a quasi-rate coefficient rather than one averaged over a Maxwellian distribution and was utilized in ultra-cold collisional studies (Krems et al. 2010; McLaughlin et al. 2014). In Fig. 7 results are shown for the radiative association rates $R(E)$ (in cm^3/s) as a function of energy expressed in temperature units (K) for the cross sections calculated for the C_2 molecule. The Deslandres-d’Azambuja ($C^1\Pi_g-A^1\Pi_u$) transitions are the main contributors for low temperature and the Radi-Bornhauser ($1^5\Pi_u-1^5\Pi_g$) bands are the main contributors for high temperatures. The Swan ($d^3\Pi_g-a^3\Pi_u$) bands also contribute to the total rate.

In Fig. 8 we compare our Maxwellian averaged quantal rates for the dominant Deslandres-d’Azambuja, Swan, and Radi-Bornhauser transitions and their sum with those determined from the previous semi-classical approximation by Andreatza & Singh (1997) over the temperature range 100-10,000 Kelvin. The quantal rates have the appropriate statistical population included so a comparison could be made directly with the previous semiclassical results of Andreatza & Singh (1997). The total rate coefficient is fit to better than 6 percent by the function

$$\alpha(T) = 5.031 \times 10^{-18} + 1.501 \times 10^{-16}T^{-1} + 2.517 \times 10^{-21}T - 1.89 \times 10^{-25}T^2 \quad \text{cm}^3/\text{s}, \quad (7)$$

$$100 \leq T \leq 10,000 \text{ K}$$

Contemporary discussions of resonances in radiative association cross sections were given by, for example, Bennett et al. (2003); Barinovs & van Hemert (2006); Bennett et al. (2008); Augustovičová

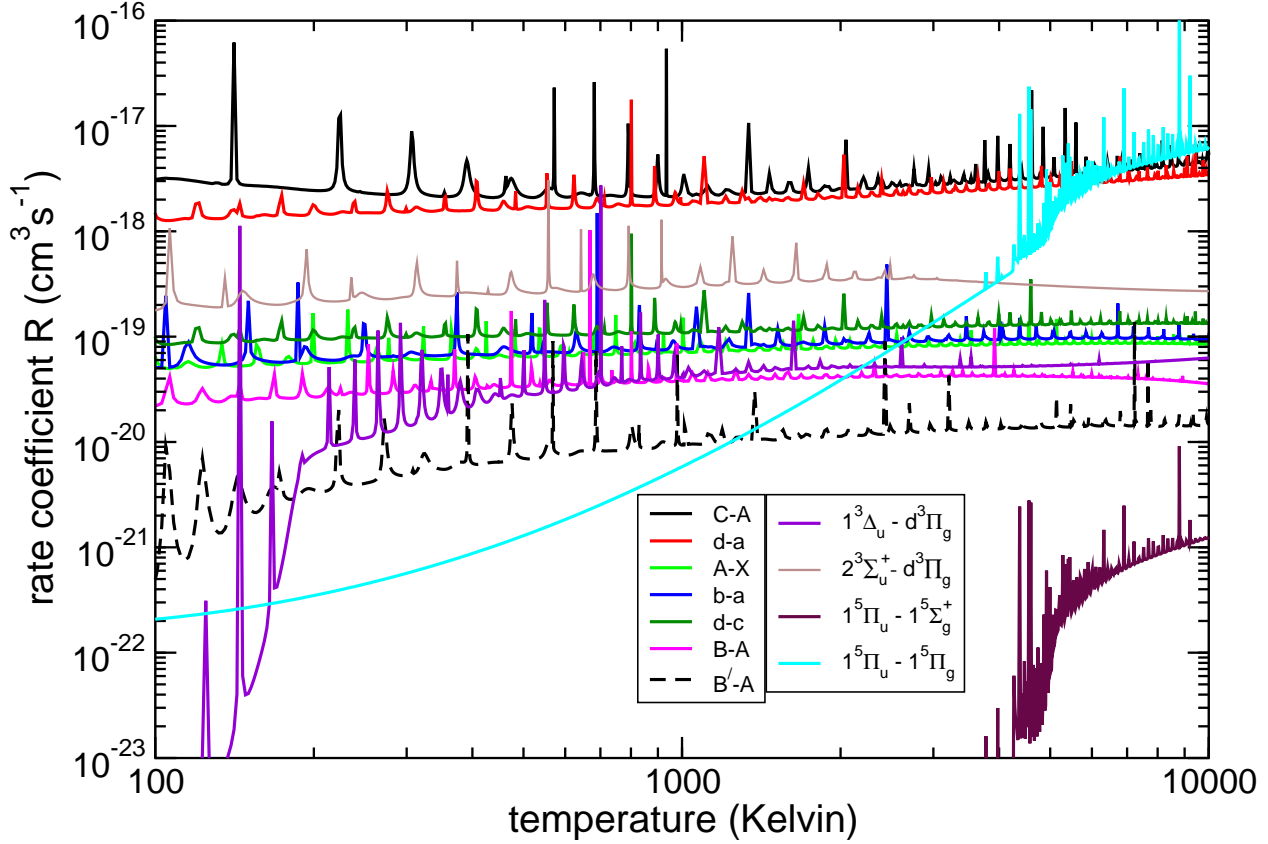


Figure 7. Radiative association quasi-energy dependent rates R (cm^3/s) as a function of effective kinetic temperature (K) for the C_2 molecule. The appropriate weighting factors, Eq. (4), are included. The Deslandres-d’Azambuja ($\text{C}^1\Pi_g\text{-A}^1\Pi_u$), and the Swan ($\text{d}^3\Pi_g\text{-a}^3\Pi_u$) bands are the major contributors to the total rate, though the Radi-Bornhauser ($1^5\Pi_u\text{-}1^5\Pi_g$) band contributes for $T > 5000$ K.

et al. (2012); Mrugała & Kraemer (2013); Golubev et al. (2013), though earlier researchers also considered the problem in detail (Giusti-Suzor et al. 1976; Flower & Roueff 1979; Graff et al. 1983), with considerations of radiative and tunneling contributions to resonance widths. Our procedures for calculating the cross sections, e.g. Eq. (2), and the corresponding rate coefficients, as shown in Fig. 8, include shape and resonance tunneling resonances. Procedures for the precision treatment of the effects of radiative decay have been developed: *i*) excise certain resonances from the cross sections, recalculate them including the sum of the partial widths for radiative decay and tunneling, and then insert them back; *ii*) add the separately calculated resonance cross sections to the semi-classical cross sections; or *iii*) add the separately calculated resonance cross sections to a background smooth base line derived from the quantum cross sections. Franz et al. (2011) and Antipov et al. (2013) examined radiative association of carbon and oxygen to form CO ($\text{A}^1\Pi\text{-X}^1\Sigma^+$), where there is a local maximum in the $\text{A}^1\Pi$ state of 0.079 eV (900 K effective temperature). Previous calculations

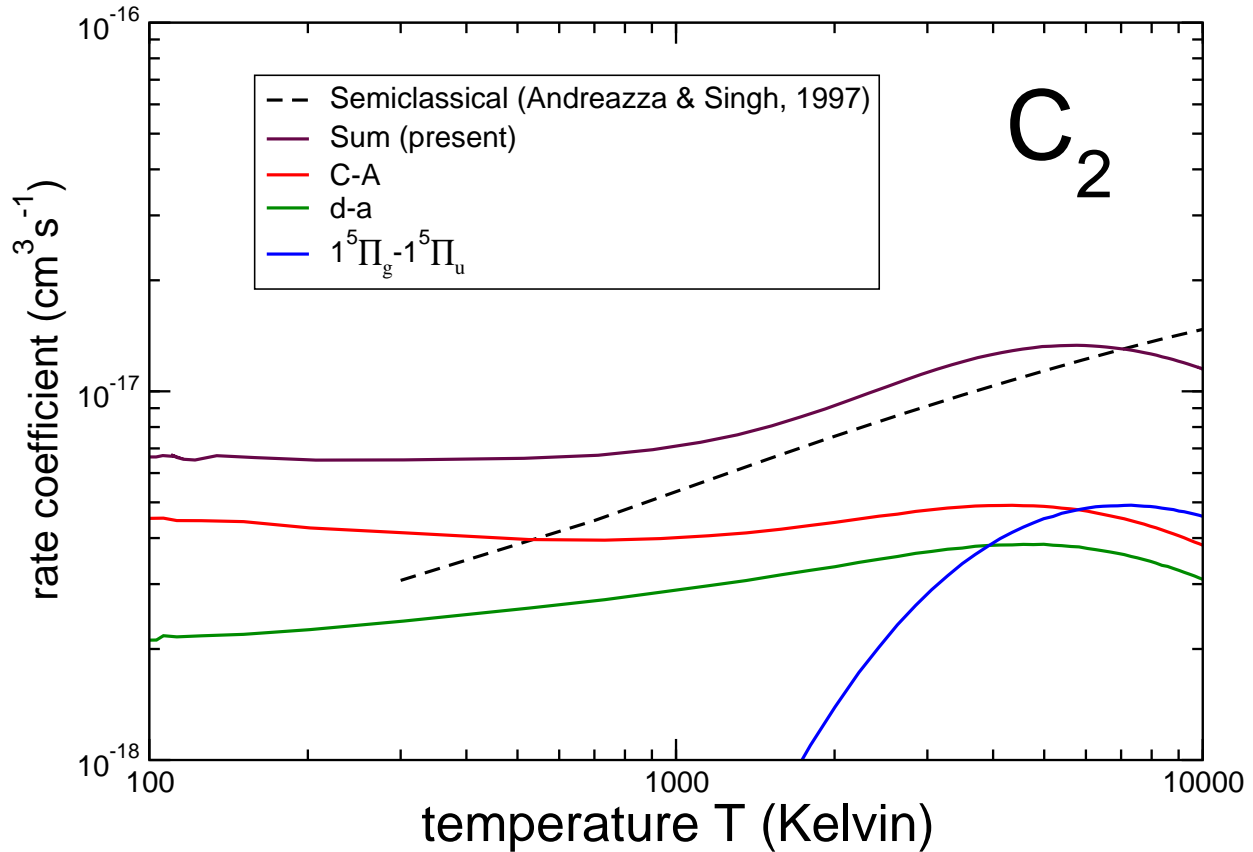


Figure 8. Maxwellian averaged radiative association rates (cm^3/s) as a function of temperature (Kelvin) for the C_2 molecule. Results are shown for the dominant singlet, triplet, and quintet transitions with their appropriate statistical factor included. The total quantal rate (brown line) is seen to lie above the previous total semiclassical rate (Andreazza & Singh 1997) (dashed black line) at all but the highest temperatures.

of rate coefficients corresponding to semi-classical cross sections (using different molecular data) were available for comparison (Dalgarno et al. 1990; Singh et al. 2002). Using the quantum-mechanical theory [our Eq. (2)], using semi-classical methods, and with specific treatment of resonances, Franz et al. (2011) and Antipov et al. (2013) found that for the rate coefficients corresponding to quantum cross sections with Eq. (2) (Franz et al. 2011) or to hybrid calculations using procedure *ii*) (semi-classical theory combined with additive quantum treatment of resonances) (Antipov et al. 2013) that resonances contribute below about 900 K. However, the rate coefficients for the quantum calculation, Fig. 2 of (Franz et al. 2011) and those for the hybrid calculations, Fig. 4a of (Antipov et al. 2013), do not deviate until the temperature is below 100 K. Precision treatment of radiative decay for the numerous resonances in our cross sections might yield enhanced values at lower temperatures, but given the application envisioned, namely to calculate corresponding rate coefficients for applications to the chemical models of supernovae ejecta, where many chemical reactions enter and few reaction

rate coefficients are known precisely and where the temperatures of interest are perhaps of order 1000-2000 K, the present procedures are satisfactory.

4. DISCUSSION

We see that our present quantal rates are larger than those from the previous semiclassical results of [Andreazza & Singh \(1997\)](#) at temperatures below 7000 K, and our quantal rates persist with a value of about $7 \times 10^{-18} \text{ cm}^3\text{s}^{-1}$ as temperatures approach 100 K. [Andreazza & Singh \(1997\)](#) listed the Swan and Deslandres-d'Azambuja transitions (in that order) as the leading contributors to the radiative association process. Our results indicate that the Deslandres-d'Azambuja transitions dominate the Swan transitions for all temperatures. [Andreazza & Singh \(1997\)](#) used a potential energy function for the C $^1\Pi_g$ state with a barrier of 0.002 eV; they did not list the cross sections, but in the semiclassical method the cross sections for C $^1\Pi_g$ -A $^1\Pi_u$ transitions would be negligible for relative energies less than effective collisional temperature of the barrier, about 25 K, so this would not affect the comparison at thermal temperatures. We note that [Andreazza & Singh \(1997\)](#) did not include quintet states (for which no experimental data were available at that time) and except for the trend towards lower temperatures, our total rate coefficient is in reasonable agreement with their calculation. We note that the $1^5\Pi_u$ - $1^5\Pi_g$ transition is the main contributor (as seen from Fig. 8) to the rate coefficient for temperatures above 5000 K.

As mentioned above, in laboratory carbon vapors generated by laser radiation, the presence of dicarbon is confirmed by, primarily, radiation from the Swan bands, but also from the Deslandres-d'Azambuja bands ([Savastenko & Tarasenko 2011](#)). In light emission from laser-induced expansion of carbon vapor from a graphite rod, [Monchicourt \(1991\)](#) found evidence of associative collisions of two ground state carbon atoms. However, the operative source of dicarbon depends on factors such as temperature and distance from the graphite substrate and there is evidence that dicarbon is formed by dissociation from the graphite ([Iida & Yeung 1994](#)) or recombination through three-body reactions ([Savastenko & Tarasenko 2011](#)). Recent modeling at certain densities of laser-induced plasmas using local thermal equilibrium and equations of states indicates C₂ may form in plasmas of Si, N, or Ar and C at characteristic temperatures roughly less than 5000 K ([Shabanov & Gornushkin 2015](#)), corresponding to the relatively low temperature region of the plasma ([De Giacomo & Hermann 2017](#)). That dicarbon is formed by a recombination process involving two carbon atoms in laser-induced plasma chemistry was shown experimentally using carbon isotopes by [Dong et al. \(2013\)](#).

The dominance of the $1^5\Pi_u$ - $1^5\Pi_g$ transitions in our calculations is interesting in light of theories of dicarbon formation in laser plasmas. In particular, [Little & Browne \(1987\)](#) theorized that the d $^3\Pi_g$ ($v = 6$) band of dicarbon is populated by recombination collisions of atomic carbon, possibly in the presence of a third body, through the $1^5\Pi_g$ state (cf. [Caubet & Dorthé \(1994\)](#)). Subsequently, [Bornhauser et al. \(2011\)](#) experimentally verified that the metastable $1^5\Pi_g$ state perturbs the d $^3\Pi_g$ state ([Bornhauser et al. 2015](#)); population of the $1^5\Pi_g$ state leads to Swan band ($v = 6$) fluorescence. Subsequent experiments demonstrated the existence of the $1^5\Pi_u$ state ([Bornhauser et al. 2015](#)). Depending on the densities and applicable chemistries of laser generated carbon vapors, the radiative association process $1^5\Pi_u$ - $1^5\Pi_g$ might contribute to the production of dicarbon in the $1^5\Pi_g$ state enhancing the mechanism of [Little & Browne \(1987\)](#).

For models of carbonaceous dust production in core-collapse supernovae, the present results provide improved rates for an initial step in carbon chain production. Our rates may be compared to rates from a kinetic theory based nucleation model ([Lazzati & Heger 2016](#)), which are a factor of 10^6 larger,

and can be applied to molecular nucleation models (Sluder et al. 2018) or chemical reaction network models (Yu et al. 2013; Clayton & Meyer 2018).

5. CONCLUSIONS

Accurate cross sections and rates for the formation of dicarbon by the radiative association process were computed for transitions from several excited electronic states using new *ab initio* potentials and transition dipole moment functions. Where calculated values exist in the literature, our TDM functions are in good agreement with previous results, but our calculations are presented over a more extensive range of internuclear distances. We also present TDM functions for the $B^1\Delta_g-A^1\Pi_u$, $d^3\Pi_g-1^3\Delta_u$, $d^3\Pi_g-2^3\Sigma_u^+$, $1^5\Pi_u-1^5\Pi_g$ (Radi-Bornhauser band), $1^5\Sigma_g^+-1^5\Pi_u$, $2^5\Sigma_g^+-1^5\Pi_u$, and $1^5\Delta_g-1^5\Pi_u$ transitions, substantially extending the available TDM data for dicarbon. We found that at the highest temperatures the quintet state Radi-Bornhauser ($1^5\Pi_u-1^5\Pi_g$) transitions are the dominant channel for radiative association, followed by the Deslandres-d’Azambuja ($C^1\Pi_g-A^1\Pi_u$) and Swan ($d^3\Pi_g-a^3\Pi_u$) transitions, while at lower temperatures the Deslandres-d’Azambuja transitions are dominant. The computed cross sections and rates for C_2 are suitable for applicability in a variety of interstellar environments including diffuse and translucent clouds and ejecta of core-collapse supernovae. In addition, our calculations do not contradict evidence that in laser ablated vapors dicarbon formation proceeds through the $1^5\Pi_g$ state. We concur with Furtenbacher et al. (2016) that further experimental studies on the Deslandres-d’Azambuja transitions are desirable.

This work was supported by a Smithsonian Scholarly Studies grant. BMMcL acknowledges support by the US National Science Foundation through a grant to ITAMP at the Center for Astrophysics | Harvard & Smithsonian under the visitor’s program, the University of Georgia at Athens for the award of an adjunct professorship, and Queen’s University Belfast for a visiting research fellowship (VRF). We thank Captain Thomas J. Lavery, USN, Ret., for his constructive comments that enhanced the quality of this manuscript. The authors acknowledge this research used grants of computing time at the National Energy Research Scientific Computing Centre (NERSC), which is supported by the Office of Science of the U.S. Department of Energy (DOE) under Contract No. DE-AC02-05CH11231. The authors gratefully acknowledge the Gauss Centre for Supercomputing e.V. (www.gauss-center.eu) for funding this project by providing computing time on the GCS Supercomputer HAZEL HEN at Höchstleistungsrechenzentrum Stuttgart (www.hlrs.de). ITAMP is supported in part by NSF Grant No. PHY-1607396.

REFERENCES

- Abellán, F. J., Indebetouw, R., Marcaide, J. M., et al. 2017, *ApJ*, 842, L24, doi: [10.3847/2041-8213/aa784c](https://doi.org/10.3847/2041-8213/aa784c)
- A’Hearn, M. F., Millis, R. C., Schleicher, D. O., Osip, D. J., & Birch, P. V. 1995, *Icarus*, 118, 223, doi: [10.1006/icar.1995.1190](https://doi.org/10.1006/icar.1995.1190)
- Amiot, C. 1983, *ApJS*, 52, 329, doi: [10.1086/190870](https://doi.org/10.1086/190870)
- Andreazza, C. M., Marinho, E. P., & Singh, P. D. 2006, *MNRAS*, 372, 1653, doi: [10.1111/j.1365-2966.2006.10964.x](https://doi.org/10.1111/j.1365-2966.2006.10964.x)
- Andreazza, C. M., & Singh, P. D. 1997, *MNRAS*, 287, 287, doi: [10.1093/mnras/287.2.287](https://doi.org/10.1093/mnras/287.2.287)
- Antipov, S. V., Gustafsson, M., & Nyman, G. 2013, *MNRAS*, 430, 946, doi: [10.1093/mnras/sts615](https://doi.org/10.1093/mnras/sts615)

- Augustovičová, L., Špirko, V., Kraemer, W. P., & Soldán, P. 2012, *Chem. Phys. Lett.*, 531, 59, doi: [10.1016/j.cplett.2012.02.038](https://doi.org/10.1016/j.cplett.2012.02.038)
- Babb, J. F., & Dalgarno, A. 1995, *PhRvA*, 51, 3021, doi: [10.1103/PhysRevA.51.3021](https://doi.org/10.1103/PhysRevA.51.3021)
- Babb, J. F., & Kirby, K. P. 1998, in *Molecular Astrophysics of Stars and Galaxies*, ed. T W Hartquist and D A Williams (Oxford, UK: Clarendon Press), 11
- Babb, J. F., & McLaughlin, B. M. 2017a, *J. Phys. B: At. Mol. Opt. Phys.*, 50, 044003, doi: [10.1088/1361-6455/aa54f4](https://doi.org/10.1088/1361-6455/aa54f4)
- . 2017b, *MNRAS*, 468, 2052, doi: [10.1093/mnras/stx630](https://doi.org/10.1093/mnras/stx630)
- . 2018, *ApJ*, 860, 151, doi: [10.3847/1538-4357/aac5f4](https://doi.org/10.3847/1538-4357/aac5f4)
- Barinovs, Ģ., & van Hemert, M. C. 2006, *ApJ*, 636, 923, doi: [10.1086/498080](https://doi.org/10.1086/498080)
- Bennett, O. J., Dickinson, A. S., Leininger, T., & Gadéa, F. X. 2008, *MNRAS*, 384, 1743, doi: [10.1111/j.1365-2966.2008.12586.x](https://doi.org/10.1111/j.1365-2966.2008.12586.x)
- Bennett, O. J., Dickinson, A. S., Leininger, T., & Gadéa, X. 2003, *MNRAS*, 341, 361, doi: [10.1046/j.1365-8711.2003.06422.x](https://doi.org/10.1046/j.1365-8711.2003.06422.x)
- Black, J. H., & Dalgarno, A. 1977, *ApJS*, 34, 405, doi: [10.1086/190455](https://doi.org/10.1086/190455)
- Boggio-Pasqua, M., Voronin, A., Halvick, P., & Rayez, J.-C. 2000, *J. Molec. Struct.: THEOCHEM*, 531, 159, doi: [10.1016/S0166-1280\(00\)00442-5](https://doi.org/10.1016/S0166-1280(00)00442-5)
- Bornhauser, P., Marquardt, R., Gourlaouen, C., et al. 2015, *JChPh*, 142, 094313, doi: [10.1063/1.4913925](https://doi.org/10.1063/1.4913925)
- Bornhauser, P., Sych, Y., Knopp, G., Gerber, T., & Radi, P. P. 2011, *JChPh*, 134, 044302, doi: [10.1063/1.3526747](https://doi.org/10.1063/1.3526747)
- Bornhauser, P., Visser, B., Beck, M., et al. 2017, *JChPh*, 146, 114309, doi: [10.1063/1.4978334](https://doi.org/10.1063/1.4978334)
- Boschen, J. S., Theis, D., Ruedenberg, K., & Windus, T. L. 2014, *Theor. Chem. Acc.*, 133, 1425, doi: [10.1007/s00214-013-1425-x](https://doi.org/10.1007/s00214-013-1425-x)
- Brault, J. W., Testerman, L., Grevesse, N., et al. 1982, *A&A*, 108, 201
- Brooke, J. S., Bernath, P. F., Schmidt, T. W., & Bacskay, G. B. 2013, *J. Quant. Spectrosc. Rad. Trans.*, 124, 11, doi: [10.1016/j.jqsrt.2013.02.025](https://doi.org/10.1016/j.jqsrt.2013.02.025)
- Bruna, P. J., & Grein, F. 2001, *Can. J. Phys.*, 79, 653, doi: [10.1139/p01-019](https://doi.org/10.1139/p01-019)
- Cairnie, M., Forrey, R. C., Babb, J. F., Stancil, P. C., & McLaughlin, B. M. 2017, *MNRAS*, 471, 2481, doi: [10.1093/mnras/stx1715](https://doi.org/10.1093/mnras/stx1715)
- Caubet, P., & Dorthé, G. 1994, *Chem. Phys. Lett.*, 218, 529, doi: [10.1016/0009-2614\(94\)00015-8](https://doi.org/10.1016/0009-2614(94)00015-8)
- Chabalowski, C. F., Peyerimhoff, S. D., & Buenker, R. J. 1983, *Chem. Phys.*, 81, 57, doi: [10.1016/0301-0104\(83\)85302-6](https://doi.org/10.1016/0301-0104(83)85302-6)
- Chaffee, F. H., J., & Lutz, B. L. 1978, *ApJ*, 221, L91, doi: [10.1086/182671](https://doi.org/10.1086/182671)
- Chang, T. Y. 1967, *Rev. Mod. Phys.*, 39, 911, doi: [10.1103/RevModPhys.39.911](https://doi.org/10.1103/RevModPhys.39.911)
- Cherchneff, I., & Dwek, E. 2009, *ApJ*, 703, 642
- Cherchneff, I., & Sarangi, A. 2011, *Proc. IAU*, 7 (S280), 228, doi: [10.1017/S1743921311025002](https://doi.org/10.1017/S1743921311025002)
- Clayton, D. D. 2013, *ApJ*, 762, 5, doi: [10.1088/0004-637X/762/1/5](https://doi.org/10.1088/0004-637X/762/1/5)
- Clayton, D. D., Deneault, E. A. N., & Meyer, B. S. 2001, *ApJ*, 562, 480, doi: [10.1086/323467](https://doi.org/10.1086/323467)
- Clayton, D. D., Liu, W., & Dalgarno, A. 1999, *Science*, 283, 1290, doi: [10.1126/science.283.5406.1290](https://doi.org/10.1126/science.283.5406.1290)
- Clayton, D. D., & Meyer, B. S. 2018, *Geochimica et Cosmochimica Acta*, 221, 47, doi: [10.1016/j.gca.2017.06.027](https://doi.org/10.1016/j.gca.2017.06.027)
- Cochran, A. L., Barker, E. S., & Gray, C. L. 2012, *Icarus*, 218, 144, doi: [10.1016/j.icarus.2011.12.010](https://doi.org/10.1016/j.icarus.2011.12.010)
- Cooley, J. W. 1961, *Math. Comp.*, 15, 363, doi: [10.2307/2003025](https://doi.org/10.2307/2003025)
- Cowan, R. D. 1981, *The Theory of Atomic Structure and Spectra* (Berkeley, California, USA: University of California Press)
- Curtis, L. J. 2003, *Atomic Structure and Lifetimes: A Conceptual Approach* (Cambridge, UK: Cambridge University Press)
- Dalgarno, A., Du, M. L., & You, J. H. 1990, *ApJ*, 349, 675, doi: [10.1086/168355](https://doi.org/10.1086/168355)
- De Giacomo, A., & Hermann, J. 2017, *J. Phys. D: Appl. Phys.*, 50, 183002, doi: [10.1088/1361-6463/aa6585](https://doi.org/10.1088/1361-6463/aa6585)
- Dong, M., Mao, X., Gonzalez, J. J., Lu, J., & Russo, R. E. 2013, *Anal. Chem.*, 85, 2899, doi: [10.1021/ac303524d](https://doi.org/10.1021/ac303524d)
- Federman, S. R., & Huntress, W. T., J. 1989, *ApJ*, 338, 140, doi: [10.1086/167187](https://doi.org/10.1086/167187)
- Flower, D. R., & Roueff, E. 1979, *A&A*, 72, 361

- Forrey, R. C., Babb, J. F., Stancil, P. C., & McLaughlin, B. M. 2016, *J. Phys. B: At. Mol. Opt. Phys.*, 49, 184002, doi: [10.1088/0953-4075/49/18/184002](https://doi.org/10.1088/0953-4075/49/18/184002)
- . 2018, *MNRAS*, 479, 4727, doi: [10.1093/mnras/sty1739](https://doi.org/10.1093/mnras/sty1739)
- Franz, J., Gustafsson, M., & Nyman, G. 2011, *MNRAS*, 414, 3547, doi: [10.1111/j.1365-2966.2011.18654.x](https://doi.org/10.1111/j.1365-2966.2011.18654.x)
- Furtenbacher, T., Szabó, I., Császár, A. G., et al. 2016, *ApJS*, 224, 44, doi: [10.3847/0067-0049/224/2/44](https://doi.org/10.3847/0067-0049/224/2/44)
- Gianturco, F. A., & Gori Giorgi, P. 1996, *PhRvA*, 54, 4073, doi: [10.1103/PhysRevA.54.4073](https://doi.org/10.1103/PhysRevA.54.4073)
- Giusti-Suzor, A., Roueff, E., & van Regemorter, H. 1976, *J. Phys. B: At. Mol. Opt. Phys.*, 9, 1021, doi: [10.1088/0022-3700/9/6/024](https://doi.org/10.1088/0022-3700/9/6/024)
- Goebel, J. H., Bregman, J. D., Cooper, D. M., et al. 1983, *ApJ*, 270, 190, doi: [10.1086/161110](https://doi.org/10.1086/161110)
- Golubev, N. V., Bezrukov, D. S., Gustafsson, M., Nyman, G., & Antipov, S. V. 2013, *J. Phys. Chem. A*, 117, 8184, doi: [10.1021/jp403174u](https://doi.org/10.1021/jp403174u)
- Graff, M. M., Moseley, J. T., & Roueff, E. 1983, *ApJ*, 269, 796, doi: [10.1086/161088](https://doi.org/10.1086/161088)
- Gredel, R., Black, J. H., & Yan, M. 2001, *A&A*, 375, 553, doi: [10.1051/0004-6361:20010769](https://doi.org/10.1051/0004-6361:20010769)
- Green, P. 2013, *ApJ*, 765, 12, doi: [10.1088/0004-637X/765/1/12](https://doi.org/10.1088/0004-637X/765/1/12)
- Grevesse, N., & Sauval, A. J. 1973, *A&A*, 27, 29
- Gustafsson, M., Antipov, S. V., Franz, J., & Nyman, G. 2012, *JChPh*, 137, 104301, doi: [10.1063/1.4750029](https://doi.org/10.1063/1.4750029)
- Helgaker, T., Jørgesen, P., & Olsen, J. 2000, *Molecular Electronic-Structure Theory* (New York, USA: Wiley)
- Herzberg, G. 1950, *Spectra of Diatomic Molecules* (New York, USA: Van Nostrand)
- Iglesias-Groth, S. 2011, *MNRAS*, 411, 1857, doi: [10.1111/j.1365-2966.2010.17807.x](https://doi.org/10.1111/j.1365-2966.2010.17807.x)
- Iida, Y., & Yeung, E. S. 1994, *Appl. Spectrosc.*, 48, 945, doi: [10.1366/0003702944029596](https://doi.org/10.1366/0003702944029596)
- Jackson, W. 1976, *J. Photochem.*, 5, 107, doi: [10.1016/0047-2670\(76\)85014-9](https://doi.org/10.1016/0047-2670(76)85014-9)
- Johnson, B. R. 1977, *JChPh*, 67, 4086, doi: [10.1063/1.435384](https://doi.org/10.1063/1.435384)
- Keenan, P. C. 1993, *PASP*, 105, 905, doi: [10.1086/133252](https://doi.org/10.1086/133252)
- Kirby, K., & Liu, B. 1979, *JChPh*, 70, 893, doi: [10.1063/1.437480](https://doi.org/10.1063/1.437480)
- Knipp, J. K. 1938, *Phys. Rev.*, 53, 734, doi: [10.1103/PhysRev.53.734](https://doi.org/10.1103/PhysRev.53.734)
- Kokkin, D. L., Bacskay, G. B., & Schmidt, T. W. 2007, *JChPh*, 126, 084302, doi: [10.1063/1.2436879](https://doi.org/10.1063/1.2436879)
- Krems, R., Friedrich, B., & Stwalley, W. C., eds. 2010, *Cold Molecules: Theory, Experiment, Applications* (Boca Raton, FL: CRC Press)
- Lambert, D. L. 1978, *MNRAS*, 182, 249, doi: [10.1093/mnras/182.2.249](https://doi.org/10.1093/mnras/182.2.249)
- Langhoff, S. R., Bauschlicher, C. W., Rendell, A. P., & Komornicki, A. 1990, *JChPh*, 92, 3000, doi: [10.1063/1.457895](https://doi.org/10.1063/1.457895)
- Lazzati, D., & Heger, A. 2016, *ApJ*, 817, 134, doi: [10.3847/0004-637X/817/2/134](https://doi.org/10.3847/0004-637X/817/2/134)
- Little, C., & Browne, P. 1987, *Chem. Phys. Lett.*, 134, 560, doi: [10.1016/0009-2614\(87\)87193-2](https://doi.org/10.1016/0009-2614(87)87193-2)
- Liu, W., & Dalgarno, A. 1995, *ApJ*, 454, 472, doi: [10.1086/176498](https://doi.org/10.1086/176498)
- Liu, W., Dalgarno, A., & Lepp, S. 1992, *ApJ*, 396, 679, doi: [10.1086/171749](https://doi.org/10.1086/171749)
- Loidl, R., Lançon, A., & Jørgensen, U. G. 2001, *A&A*, 371, 1065, doi: [10.1051/0004-6361:20010400](https://doi.org/10.1051/0004-6361:20010400)
- Lord, III, H. C. 1965, *Icarus*, 4, 279, doi: [10.1016/0019-1035\(65\)90005-9](https://doi.org/10.1016/0019-1035(65)90005-9)
- Macrae, R. M. 2016, *Sci. Prog.*, 99, 1, doi: [10.3184/003685016X14509452393033](https://doi.org/10.3184/003685016X14509452393033)
- Martin, M. 1992, *J. Photochem. Photobio. A: Chem.*, 66, 263, doi: [10.1016/1010-6030\(92\)80001-C](https://doi.org/10.1016/1010-6030(92)80001-C)
- McLaughlin, B. M., Lamb, H. D. L., Lane, I. C., & McCann, J. F. 2014, *J. Phys. B: At. Mol. Opt. Phys.*, 47, 145201, doi: [10.1088/0953-4075/47/14/145201](https://doi.org/10.1088/0953-4075/47/14/145201)
- McMillan, E. C., Shen, G., McCann, J. F., McLaughlin, B. M., & Stancil, P. C. 2016, *J. Phys. B: At. Mol. Opt. Phys.*, 49, 084001, doi: [10.1088/0953-4075/49/8/084001](https://doi.org/10.1088/0953-4075/49/8/084001)
- Messerle, G., & Krauss, L. 1967, *Z. Natur. A*, 22, 2015, doi: [10.1515/zna-1967-1225](https://doi.org/10.1515/zna-1967-1225)
- Millar, T. J., Bennett, A., Rawlings, J. M. C., Brown, P. D., & Charnley, S. B. 1991, *A&AS*, 87, 585
- Miller, J. H., & Kelly, H. P. 1972, *Phys. Rev. A*, 5, 516, doi: [10.1103/PhysRevA.5.516](https://doi.org/10.1103/PhysRevA.5.516)
- Monchicourt, P. 1991, *PhRvL*, 66, 1430, doi: [10.1103/PhysRevLett.66.1430](https://doi.org/10.1103/PhysRevLett.66.1430)
- Mrugała, F., & Kraemer, W. P. 2013, *JChPh*, 138, 104315, doi: [10.1063/1.4793986](https://doi.org/10.1063/1.4793986)

- Nemes, L., & Irle, S., eds. 2011, Spectroscopy, Dynamics and Molecular Theory of Carbon Plasmas and Vapors (Singapore: World Scientific)
- ONeil, S. V., Rosmus, P., & Werner, H. 1987, JChPh, 87, 2847, doi: [10.1063/1.453072](https://doi.org/10.1063/1.453072)
- Pattillo, R. J., Cieszewski, R., Stancil, P. C., et al. 2018, ApJ, 858, 10, doi: [10.3847/1538-4357/aab5b9](https://doi.org/10.3847/1538-4357/aab5b9)
- Prasad, S. S., & Huntress, W. T. 1980, ApJS, 43, 1, doi: [10.1086/190665](https://doi.org/10.1086/190665)
- Rho, J., Geballe, T. R., Banerjee, D. P. K., et al. 2018, ApJ, 864, L20, doi: [10.3847/2041-8213/aad77f](https://doi.org/10.3847/2041-8213/aad77f)
- Sarangi, A., & Cherchneff, I. 2013, ApJ, 776, 107, doi: [10.1088/0004-637X/776/2/107](https://doi.org/10.1088/0004-637X/776/2/107)
- Sarangi, A., Matsuura, M., & Micelotta, E. R. 2018, SSRv, 214, 63, doi: [10.1007/s11214-018-0492-7](https://doi.org/10.1007/s11214-018-0492-7)
- Savastenko, N. A., & Tarasenko, N. V. 2011, in Spectroscopy, Dynamics and Molecular Theory of Carbon Plasmas and Vapors, ed. L. Nemes & S. Irle (Singapore: World Scientific), 167–198
- Schmidt, T. W., & Bacskay, G. B. 2011, JChPh, 134, 224311, doi: [10.1063/1.3599933](https://doi.org/10.1063/1.3599933)
- Shabanov, S. V., & Gornushkin, I. B. 2015, Appl. Phys. A, 121, 1087, doi: [10.1007/s00339-015-9445-0](https://doi.org/10.1007/s00339-015-9445-0)
- Shen, G., Stancil, P. C., Wang, J. G., McCann, J. F., & McLaughlin, B. M. 2015, J. Phys. B: At. Mol. Opt. Phys., 48, 105203, doi: [10.1088/0953-4075/48/10/105203](https://doi.org/10.1088/0953-4075/48/10/105203)
- Singh, P. D., Sanzovo, G. C., Borin, A. C., & Ornellas, F. R. 2002, MNRAS, 303, 235, doi: [10.1111/j.1365-2958.2008.06311.x-i1](https://doi.org/10.1111/j.1365-2958.2008.06311.x-i1)
- Sluder, A., Milosavljević, M., & Montgomery, M. H. 2018, MNRAS, 480, 5580, doi: [10.1093/mnras/sty2060](https://doi.org/10.1093/mnras/sty2060)
- Tanabashi, A., Hirao, T., Amano, T., & Bernath, P. F. 2007, ApJS, 169, 472, doi: [10.1086/510742](https://doi.org/10.1086/510742)
- Tsuji, T. 1964, Ann. Tokyo Astron. Observ., 2nd. Ser., 9, 1
- van Dishoeck, E. F., & Black, J. H. 1989, ApJ, 340, 273, doi: [10.1086/167391](https://doi.org/10.1086/167391)
- van Dishoeck, E. F., Blake, G. A., Draine, B. T., & Lunine, J. I. 1993, in Protostars and Planets III, ed. E. H. Levy & J. I. Lunine (Tucson: University of Arizona Press), 163
- Varandas, A. J. C. 2008, JChPh, 129, 234103, doi: [10.1063/1.3036115](https://doi.org/10.1063/1.3036115)
- Varandas, A. J. C., & Rocha, C. M. R. 2018, Philos. Trans. Royal Soc. A, 376, 20170145, doi: [10.1098/rsta.2017.0145](https://doi.org/10.1098/rsta.2017.0145)
- Visser, B., Beck, M., Bornhauser, P., et al. 2019, Molec. Phys., online Jan. 22, 2019, doi: [10.1080/00268976.2018.1564849](https://doi.org/10.1080/00268976.2018.1564849)
- Watson, J. K. G. 2008, J. Mol. Spec., 253, 5, doi: [10.1016/j.jms.2008.04.014](https://doi.org/10.1016/j.jms.2008.04.014)
- Werner, H.-J., Knowles, P. J., Knizia, G., Manby, F. R., & Schütz, M. 2012, WIREs Comput. Mol. Sci., 2, 242, doi: [10.1002/wcms.82](https://doi.org/10.1002/wcms.82)
- Werner, H.-J., Knowles, P. J., Knizia, G., et al. 2015, MOLPRO, version 2015.1, a package of *ab initio* programs. <http://www.molpro.net>
- Yu, T., Meyer, B. S., & Clayton, D. D. 2013, ApJ, 769, 38, doi: [10.1088/0004-637X/769/1/38](https://doi.org/10.1088/0004-637X/769/1/38)
- Yurchenko, S. N., Szabó, I., Pyatenko, E., & Tennyson, J. 2018, MNRAS, 480, 3397, doi: [10.1093/mnras/sty2050](https://doi.org/10.1093/mnras/sty2050)
- Zhang, X.-N., Shi, D.-H., Sun, J.-F., & Zhu, Z.-L. 2011, Chin. Phys. B, 20, 043105, doi: [10.1088/1674-1056/20/4/043105](https://doi.org/10.1088/1674-1056/20/4/043105)